Talanta 85 (2011) 2445–2450

Contents lists available at ScienceDirect

Talanta

journal homepage: www.elsevier.com/locate/talanta

Modified interdigitated arrays by novel poly(1,8-diaminonaphthalene)/carbon nanotubes composite for selective detection of mercury(II)

Dzung Tuan Nguyen[a,1], Lam Dai Tran[b,*,1], Huy Le Nguyen[c], Binh Hai Nguyen[b], Nguyen Van Hieu[d]

[a] Institute of Tropical Technology, Vietnam Academy of Science and Technology, 18 Hoang Quoc Viet Road, Hanoi, Viet Nam
[b] Institute of Materials Science, Vietnam Academy of Science and Technology, 18 Hoang Quoc Viet Road, Hanoi, Viet Nam
[c] School of Chemical Engineering, Hanoi University of Science and Technology, 1, Dai Co Viet Road, Hanoi, Viet Nam
[d] International Training Institute for Materials Science, Hanoi University of Science and Technology, 1, Dai Co Viet Road, Hanoi, Viet Nam

ARTICLE INFO

Article history:
Received 14 March 2011
Received in revised form 27 July 2011
Accepted 27 July 2011
Available online 5 August 2011

Keywords:
Poly(1,8-diaminonaphthalene) (PDAN)
Functionalized multi-walled carbon nanotubes (CNT)
Interdigitated arrays (IDA)
Square wave voltammetry (SWV)
Mercury selective detection

ABSTRACT

This study describes a novel type of interdigitated arrays (IDA), microfabricated by electropolymerizing structured Poly(1,8-diaminonaphthalene)/functionalized multi-walled carbon nanotubes (PDAN/CNT) thin film onto a silicon chip for square wave voltammetry (SWV) multi-element heavy metal ion detection. The structure of PDAN/CNT was characterized by Raman, FE-SEM and AFM techniques. Analysed experiments reveal that the uptake of Hg^{2+} by PDAN/CNT is quite specific and it can be used advantageously for electrochemical sensing of Hg^{2+} thanks to original feature of (Hg^{2+}/Hg_2^{2+}) redox potential with the respect to that of PDAN/CNT. As-developed IDA type electrode can extend its utility in other sensing applications.

1. Introduction

Contamination of the environment with heavy metal ions especially by mercury ions has drawn a considerable concern worldwide. As mercury can accumulate in the vital organs and tissues to bind with sulfur-containing proteins and enzymes, some important cell functions are inactivated which lead to a wide variety of diseases [1]. The US Environmental Protection Agency (EPA) limit of Hg(II) for drinkable water is 10 nM which is much lower than the detection limit of most available assays [2]. Therefore, development of a simple/economical, but sensitive/selective as well as practical/label-free method is highly demanded for environmental monitoring, food industry and clinical diagnostics [3,4]. Optical methods of analysis like atomic absorption spectrophotometry (AAS), conventional analytical techniques such as inductively coupled plasma-atomic emission spectroscopy (ICP-AES) and inductively coupled plasma-mass spectrometry (ICP-MS), X-ray fluorescence (XRF), neutron activation analysis (NAA) are powerful techniques but they are complex, expensive and thus are not practical for routine monitoring of Hg(II). Another alternative of optical sensing systems for the detection of Hg(II) could be also based on organic chromophores or fluorophores, biomolecules such as proteins, antibodies, oligonucleotides, DNAzymes and semiconductor quantum dots, conjugated polymers and gold nanoparticles and other inorganic materials. However, poor selectivity, inefficient sensitivity and stability are some limitations with most of these methods for on-site screening. Therefore, it is critical to develop simpler and more practical techniques to detect Hg^{2+}. For this purpose, anodic stripping voltammetry (ASV) is a voltammetric method for quantitative determination of specific ionic species. The analyte of interest is electroplated on the working electrode during a deposition step, and oxidized from the electrode during the stripping step. The current is measured during the stripping step. The oxidation of species is registered as a peak in the current signal at the potential at which the species begins to be oxidized. The stripping step can be either linear, staircase, square wave, or pulse. Traditionally, electrodes modified with a mercury film on a glassy carbon electrode has been effectively used in ASV [5]. It is a convenient and highly sensitive technique based on the ability of mercury to form amalgams with other metals during a preconcentration step. However, it is important to mention that Hg vapors are very poisonous besides Hg itself is considered to be one of the major pollutants of the environment. Therefore, in recent years, ASV is used in conjunction with the use of other chemically modified electrodes, among which nanosize material becomes a promising alternative for modification of electrodes in the electroanalysis of Hg(II) [6–8].

* Corresponding author. Tel.: +84 4 37564129; fax: +84 4 38360705.
E-mail address: lamtd@ims.vast.ac.vn (L.D. Tran).
[1] These authors equally contributed to this paper.

0039-9140/$ – see front matter © 2011 Elsevier B.V. All rights reserved.
doi:10.1016/j.talanta.2011.07.094

In other aspect, as for electrode materials, electronically conducting polymer films have been paid great attention in the past two decades, due to their unique physical and chemical properties and some potential applications in batteries, microelectronic and electrocatalytic devices [9]. Among those, polydiaminonaphthalene (PDAN), synthesized from aromatic diamine is a new type of multifunctional polymer following polyaniline and polypyrrole. Besides good electroconductivity, electroactivity, electrochromism and electrocatalysis, PDAN exhibits some other interesting properties that originate from chemical reactivity of functional amino groups on polymeric structure. As a new functionality, PDAN possesses chelating properties and/or reduction properties owing to the electron donating groups (amine and secondary amino groups) on the polymer chain [10,11]. It has been demonstrated that PDAN is sensitive to heavy metal ions, and able to extract some heavy metal ions including Ag^{+}, Cu^{2+}, Hg^{2+}, Pb^{2+}, VO^{2+}, Cr^{3+} from their dilute solutions at the ion concentration down to 1 μM via complexation with amine groups on the polymer [12,13]. Thus the PDAN film proved to be used as modified electrode for collecting metal ions for anodic stripping analysis of trace amount of metal ions. However, the specificity of particular ligands towards target Hg(II) resulting from a conventional acide-base complexation interaction between the ligands and Hg(II) is usually unremarkable because the other soft Lewis acids (such as Cd(II), Zn(II), Cu(II), and Ag(I)) also can interfere. Second, the PDAN film has relatively low specific area and restrictive sites to contact with metal ions, thus, it could not applied efficiently for recovery of metal ions from aqueous solutions. Effectively, to overcome the second drawback, some metal oxide nanoparticles such as iron oxide (Fe_3O_4) and zinc oxide (ZnO), carbon nanotube (CNT) and very recently graphene having a large surface-to-volume ratio, high surface reaction activity, high catalytic efficiency and strong adsorption ability were proved to be useful for improving sensor stability and sensitivity [14–16]. Among above mentioned materials, CNT will be considered as one of the most interesting materials due to its excellent characteristics including its high conductivity.

According to the available literature, to the best of our knowledge there is no previous report on the design of PDAN/CNT based IDA electrodes and the electrochemical detection of Hg^{2+} by SWV. Thus, primary objective of this work is to construct nanocomposite of PDAN/CNT to reach higher sensitivity, selectivity and also lower detection limit for mercury determination. A sensitive interface for electrochemically multiplexed analyses of heavy metal ions will be designed. Several advantageous features of our platform can be listed below: (i) IDA is attractive for their possibility to eliminate the main drawbacks of the electrochemical sensors such as the phenomenon of "electrode fouling", "memory effect" from one sample to another as well as the possibility to be produced inexpensively at large scale; (ii) designed hybrid organic–inorganic electrode interface is expected to express a synergic effect to the overall system and thus improve sensing characteristics; (iii) thanks to sensitive interface of PDAN/CNT as well as the oxidizing characteristic of ($Hg^{2+}/Hg_2{}^{2+}$) redox couple, much more positive working potential range (0.0 V to +0.7 V), compared to that normally used in typical ASV for Hg^{2+} (from −0.5 V to −1 V to +0.7 V). It will make the electrochemical detection of Hg^{2+} much more selective when the reduction of other interference divalent ions such as Cu^{2+}, Co^{2+}, Zn^{2+} and Fe^{2+} can be greatly avoided.

2. Experimental

2.1. Chemicals

All the chemicals used were of analytical grade. The 1,8-diaminonaphthalene (denoted as DAN, Merck), $HClO_4$, $NaClO_4$ (Sigma) were used without further purification. The electrochemical polymerization of PDAN was carried out by electro-oxidation of 10^{-3} M of DAN in 1 M of $HClO_4$ solution, with a scan rate of 50 mV s^{-1}. Multi-walled carbon nanotubes (CNTs) were produced by chemical vapor deposition (CVD) and exist as agglomerates. Therefore, CNTs were functionalized to enhance their dispersion in the solvent. The functionalization procedure was typical: CNTs were suspended in a mixture of concentrated H_2SO_4/HNO_3 (3/1, v/v) and refluxed for 12 h in a silicone oil bath maintained at 120 °C. The excess of acid and water was removed by filtration (Millipore, 0.5 μm). The black solid was washed thoroughly with D.I. water until neutrality of the eluent was reached. As-obtained functionalized CNTs were dried under vacuum at room temperature.

2.2. Electrode fabrication

The interdigitated electrodes arrays (IDA) was fabricated on silicon substrate via lithography technique (Fig. S1, supporting information). Silicon wafers were covered with a layer of SiO_2 1 μm thick by means of dry thermal oxidation. The wafer was spin-coated with a layer of photoresist AZ5214E (1 μm thickness) and the shape of the electrodes was defined by UV-photolithography. Then, Cr and Pt were sputtered on the top of the wafer with the thickness of 50 and 500 nm, respectively. The working and counter electrodes were patterned by a lift-off process (30 s in acetone solution with ultrasonic vibration) as shown in Fig. S1(b). A second photolithographic step is carried out to deposit the silver layer. Next, a 50 mM solution of $FeCl_3$ (Merck) was applied to the silver surface for 50 s at room temperature, followed by rinsing with DI water to define the reference electrodes. The final diameter of the working electrodes was 500 μm.

Electropolymerization of PDAN and PDAN/CNT on IDA was carried out in 0.1 M $HClO_4$ solution containing (10^{-3} M DAN) and (10^{-3} M DAN + 0.01% functionalized CNTs), respectively by using AUTOLAB PGSTAT 30 Electrochemical Analyser (EcoChemie, the Netherlands) under the control of GPES version 4.9. The parameters for CV: scan rate: 50 mV s^{-1}; the potential range for electropolymerization is between −0.15 and +1.0 V vs. SCE.

2.3. Ion metal adsorption

During adsorption step IDA electrode is immersed in the sample solution for 15 min at open circuit potential of PDAN/CNT (E_{ocp} = +0.35 V vs. SCE). Then the electrode is rinsed thoroughly with D.I water and ethanol to remove completely M^{2+} salts before further SWV experiments in M^{2+} free solutions (detection step). The adsorption step is normally carried out at room temperature for all metal ions except for Cu^{2+} (more elevated temperature (80 °C) was needed).

2.4. Characterizations (FE-SEM, AFM, IR, Raman analyses)

As-synthesized PDAN/CNTs on IDA electrodes were rinsed first with D.I. water and then with ethanol before further characterizations.

Infra red (IR) spectra were recorded with Nicolet 6700 FT-IR Spectrometer. Field Emission Scanning Electron Microscope (FE-SEM) image was analysed with Hitachi S-4800 and JEM-1200EX. Room-temperature Raman analysis was carried out with LABRAM-1B (France), with 632.8 nm laser red line (6 mW). The AFM morphology was observed by using 5500 AFM/SPM (Agilent Inc.) in tapping mode, scan speed of 1 μm s^{-1}, resonance frequency of 332 kHz.

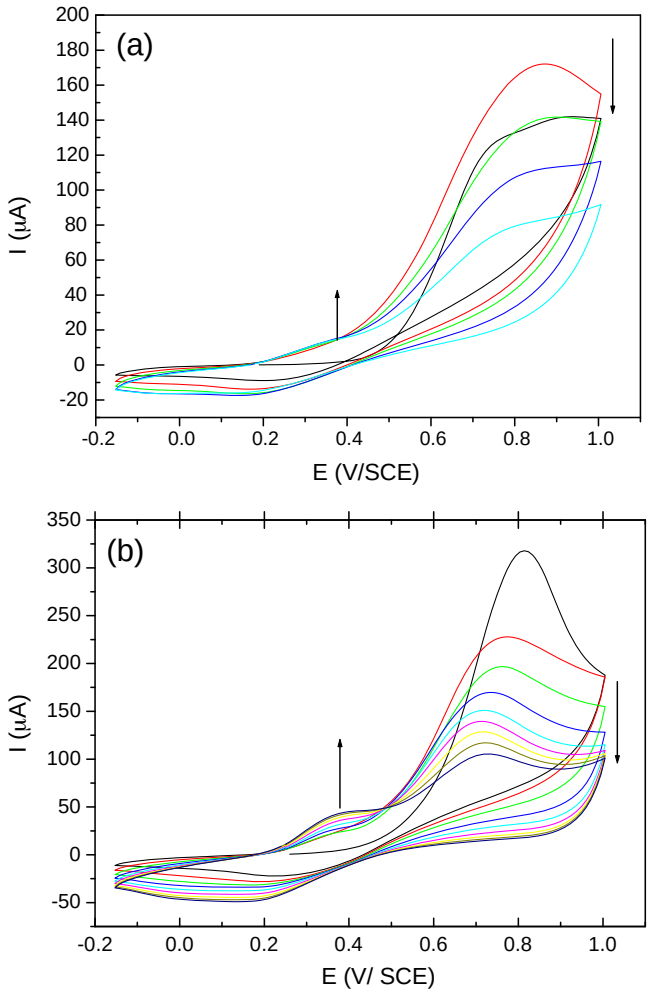

Fig. 1. Cyclic voltammograms (CVs), registered during electropolymerization of PDAN (a) and PDAN/CNT (b) on IDA in 0.1 M $HClO_4$ solutions containing (10^{-3} M DAN) and (10^{-3} M PDAN + 0.01% functionalized CNT).

2.5. Hg^{2+} detection and interfering tests by SWV

Voltammetric SWV measurements were performed on AUTOLAB PGSTAT 30 Electrochemical Analyser (EcoChemie, the Netherlands) under the control of GPES version 4.9. The parameters for SWV were optimized as follows: frequency: 12.5 Hz; start potential: 0.0 V; end potential: +0.7 V; step: 8 mV; amplitude: 25 mV. Prior to SWV measurements, the electrodes were held for 20 s at the starting potential (0.0 V) for conditioning. For interfering tests, 6 solutions containing M^{2+} ions (M^{2+} = Cu^{2+}, Hg^{2+}, Cd^{2+}, Co^{2+}, Zn^{2+}, Fe^{2+}, $[M^{2+}] = 10^{-6}$ M) and 2 blank references (H_2O and $HClO_4$) were dropped onto PDAN/CNT-modified 8 electrode IDA, and were held for 15 min. Then, M^{2+} salts were removed by accurate washing in D.I. water and ethanol (cleaning step) before further experiments according to above SWV detection protocol in M^{2+} free solution (detection step).

3. Results and discussion

3.1. Electrochemical synthesis of PDAN/CNT

Fig. 1(a) and (b) shows the cyclic voltammograms (CVs) taken during the course of electropolymerization of PDAN and PDAN/CNT on IDA respectively, as described in Section 2.2. The anodic peak, appeared in the first scan at *ca.* 0.8 V was ascribed to the oxidation

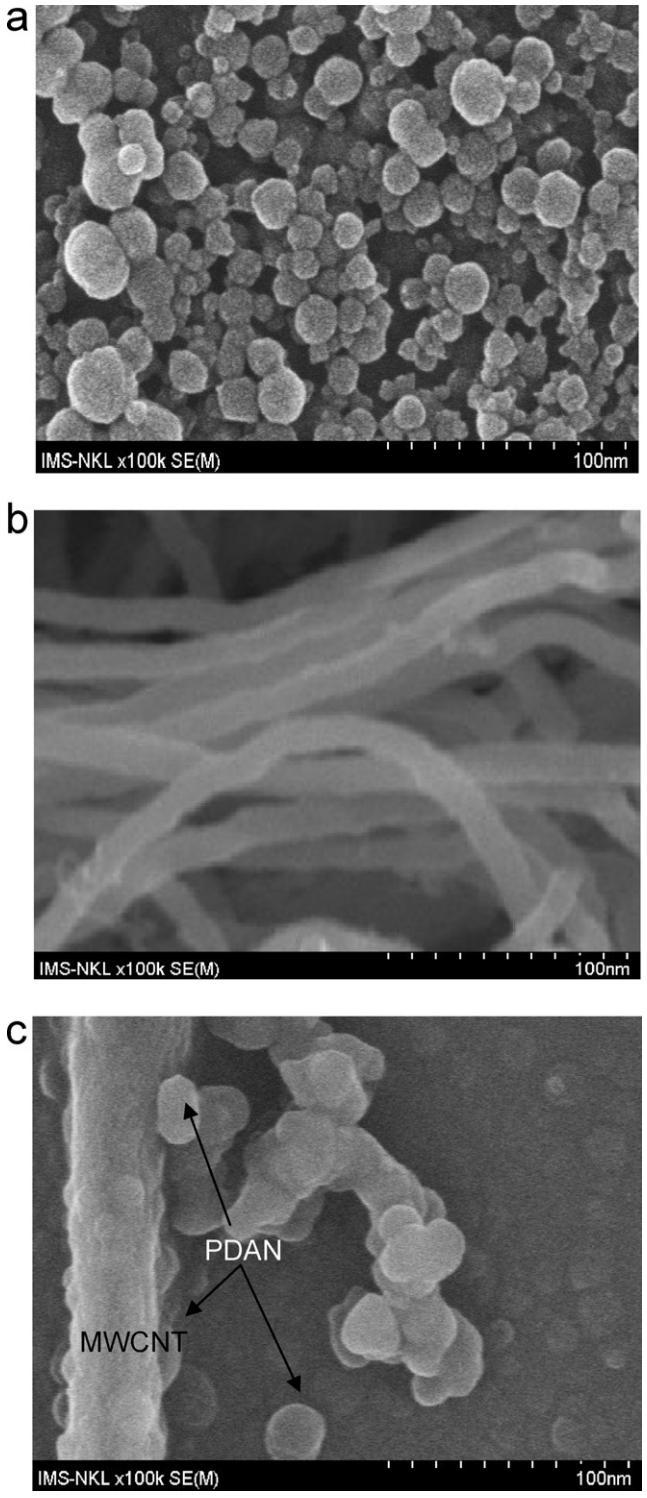

Fig. 2. FESEM images of PDAN (a); pure CNT (b) and PDAN/CNT (c).

of DAN. Successive cycling decreases the intensity of this peak (and shifts it to more negative position) but increases that of another Redox system (E_{pa} = 0.35 V and E_{pc} = 0.15 V), indicating the enhancing conductivity/electroactivity of PDAN/CNT compared to that of pure PDAN. This phenomenon was also confirmed by the fact that the oxidation current of PDAN/CNT was saturated after 9 scans, instead of 4 in case of pure PDAN.

To establish the probable structure of PDAN/CNT, IR spectrum was recorded (figure not shown). In this figure, a very broad multi-

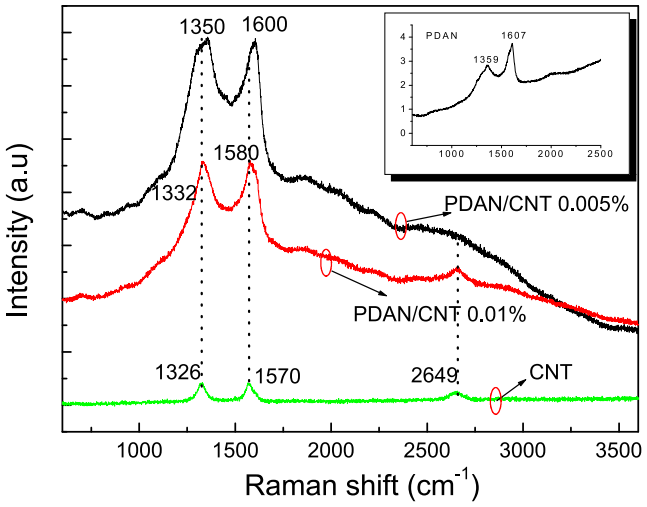

Fig. 3. Raman spectra of PDAN (inset), CNT and PDAN/CNT films.

component band with a maximum at 3403 cm^{-1}, probably formed by a mixture of primary and secondary amines was observed. Among them the most important vibration is that of amine N–H stretching since this fingerprint vibration is characteristic for polymerization reaction via –NH–NH–bond [10,11].

3.2. Film characterizations by FE-SEM and AFM

Field emission scanning electron microscopy (FE-SEM) images showed nanostructured film of pure PDAN, consisting of spherical PDAN particles of 70–100 nm in diameter (Fig. 2(a)). As for PDAN/CNT (Fig. 2(c)), it summarized the morphology of particle- and tube-forms of both PDAN and CNT (Fig. 2(b)), respectively. AFM images also bring additional evidence that the PDAN was coated/bound on the CNTs (Fig. S2, supporting information).

To further confirm the interaction between PDAN and CNTs, Raman spectra were also carried out. First, it was found that while CNTs could not be detected in IR spectra (due to such a low content of CNT (0.005–0.01%), beyond the detection range in IR method), it can be clearly seen bound on PDAN in Raman spectra (Fig. 3). Second, while pure CNTs represent D-band and G-band (at 1326 cm^{-1} and 1570 cm^{-1} respectively, due to the sp^2 sites from carbon structures) and the second-order harmonic D′ band at 2649 cm^{-1} (inset in Fig. 3) [9], pure PDAN shows a strong band and a weak band at 1607 cm^{-1} and 1359 cm^{-1}, assigned to skeletal vibration of naphthalene ring and C–N stretching vibration of polaronic units respectively [13]. Furthermore, the intensity of C–N stretching becomes more important in PDAN/CNTs, indicating a more polarized state (or higher electroactive) of PDAN/CNTs compared to that of pure PDAN. It can be expected that a strong interaction between CNT and PDAN will facilitate effective degree of electron delocalization, which in its turn, will induce an enhancement in electron transfer and thus selectivity of electrochemical detection with PDAN/CNTs interface compared to that of pure PDAN.

3.3. Selectivity detection of Hg^{2+} ions

In order to investigate the selectivity of PDAN film towards Hg^{2+}, batch experiments were done for a series of interference divalent ions such as Cu^{2+}, Hg^{2+}, Cd^{2+}, Co^{2+}, Zn^{2+}, Fe^{2+}, adsorbed on the surface of IDA at the open circuit potential of PDAN/CNT (0.35 V vs. SCE), as described in Section 2.3. After this adsorption step, in order to detect PDAN/CNT-M^{2+} complexation, SWVs were recorded for the potential range from 0 to 0.7 V vs. SCE, in metal ion free solution ($HClO_4$ 0.1 M). Some observations can be made. First, SQW curves indicated that PDAN film is not electroactive

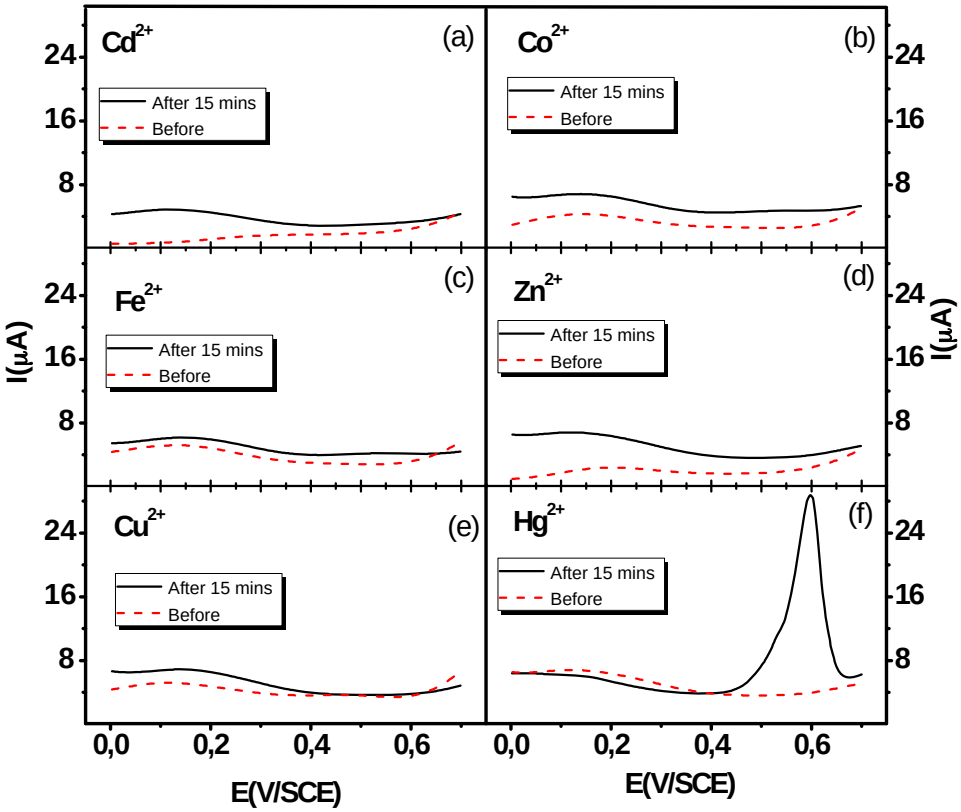

Fig. 4. SWV curves, registered during Cd^{2+}, Co^{2+}, Fe^{2+}, Zn^{2+}, Cu^{2+} and Hg^{2+} detection (corresponding to images (a), (b), (c), (d), (e) and (f) respectively).

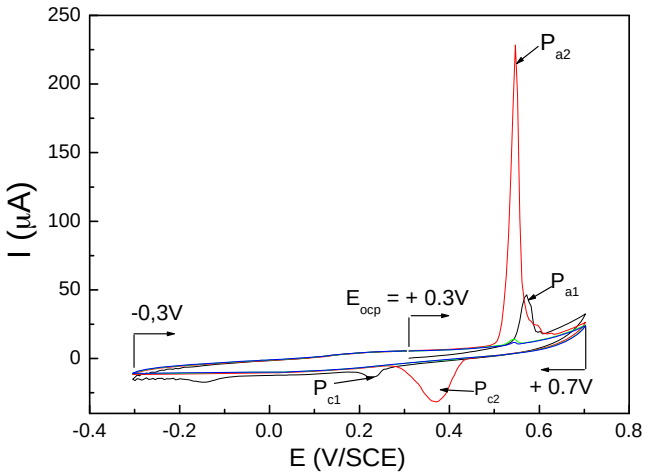

Fig. 5. CVs of PDAN/CNT, registered after accumulation step (in $HgCl_2$ 10^{-5} M).

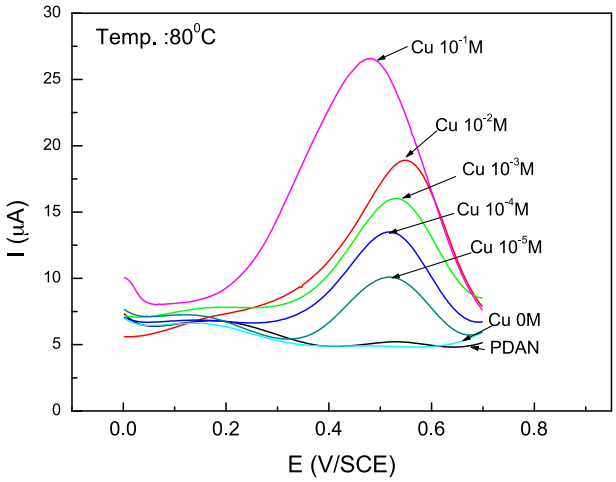

Fig. 6. SWV curves, registered during Cu^{2+} detection, after accumulation step at elevated temperature (80 °C).

in that solution (Fig. 4, dash line). Second, although PDAN did complex with M^{2+} cations (amino and/or imino groups which do not participate in PDAN polymerization are capable of forming a complexation with above mentioned M^{2+} and therefore accumulating them) their detection is impossible (a negligible SWV signal was detected for Cd^{2+}, Co^{2+}, Fe^{2+}, Zn^{2+}, Cu^{2+}, corresponding to Fig. 4(a)–(e) respectively). Third, a bias of 0.0 V in conditioning step during 20 s, is completely not enough to reduce Hg^{2+} (as well as other metals ions M^{2+}) and deposit it onto the electrode surface of PDAN/CNT [17–19]. Thus, the SWV peak in Fig. 4(f) cannot be Hg stripping as it was usually explained in ASV method. Actually, for ASV, the potential range should be imposed much more negatively, taking into account E^0 value of above mentioned metals, namely: $E^0_{Cd_{2+}/Cd} = -0.641$ V; $E^0_{Co_{2+}/Co} = -0.518$ V; $E^0_{Fe_{2+}/Fe} = -0.681$ V; $E^0_{Zn_{2+}/Zn} = -1.01$ V; $E^0_{Cu_{2+}/Cu} = +0.101$ V (vs. SCE). Forth, the fact that only Hg^{2+} can be notably detected by SWV at room temperature in this potential range (0 to +0.7 V), suggests that high value of $E^0(Hg^{2+}/Hg_2{}^{2+} = +0.67$ V) may be an important reason that makes the Hg detection: (i) different from that of other M^{2+}; (ii) possible and selective at room temperature.

To more elucidate this phenomenon, cyclic voltammograms of PDAN/CNT after adsorption step in $HgCl_2$ 10^{-5} M were recorded (Fig. 5). Starting from open circuit open (+0.35 V), the potential is swept to +0.7 V before reversing to −0.3 V. Effectively, taking into account the fact that redox potential of Hg^{2+} ($E^0(Hg^{2+}/Hg_2{}^{2+}) = +0.67$ V (vs. SCE) is considerably higher than E_{redox} of PDAN/CNT, so the polymer is supposed to be partially oxidized by means of Hg^{2+} ions (trapped in the polymer matrix after adsorption step) when the latter is reduced to $Hg_2{}^{2+}$, to form a complex of $[Hg_2{}^{2+}\cdots(PDAN/CNT)^{\bullet+}]_{el}$ at the surface of the electrode. The existence of this complex was first indicated by Jackowska's group using IR, Raman, EPR and open circuit potential measurement [20–22]. Anodic peak located at 0.57 V at the first scan (+0.35 V up to +0.7 V) was therefore attributed to the anodic electrooxidation of as-formed $Hg_2{}^{2+}$ (in the complex) into Hg^{2+} ions. After the first scan, thanks to gained electroactive/electroconductive property of PDAN/CNT, majority of Hg^{2+} ions, especially those are located/trapped deeply inside the matrix of the bulk PDAN/CNT, were capable of being electroreduced (to the $Hg_2{}^{2+}$ form). As a result of more accumulated concentration of $Hg_2{}^{2+}$, the anodic peak of +0.55 V of the second scan became much more intensive compared to that of the first scan. Above mentioned phenomenon of increasing electroconductivity of PDAN/CNT after the second scan, related to easier electron transfer within polymer backbone and/or its matrix and thus induced more favorable reduction to $Hg_2{}^{2+}$, was additionally supported by the peak intensities and peak shifts (towards more energetically favorable potentials, *i.e.* more negative and positive potentials for the oxidation and the reduction respectively) of P_{a2}, P_{c2} compared to P_{a1}, P_{c1} (P_{ai}, P_{ci} are anodic and cathodic peaks after i-th scan respectively). Moreover, the cathodic peaks (broader than the anodic ones) were registered at around +0.25 V and +0.37 V, corresponding to P_{c1} (of the first scan) and P_{c2} (of the second scan) respectively. Theoretically, mercury, like other 3d metal, such as copper, cadmium or zinc has poorly defined reduction waves, while showing sharp and intense reoxidation stripping waves [23]. Stripping peak almost disappears after the third scan, as experimentally observed in Fig. 5, was explained by the fact that after the second anodic electrooxidation wave Hg^{2+} ions will leave the electrode surface and go definitively into the solution. In summary, after adsorption step owing to chelating complexation (common feature of M^{2+} ions), the selective electrochemical detection of Hg^{2+} can occur owing to its characteristic value of ($E^0(Hg^{2+}/Hg_2{}^{2+})$ that triggered $Hg^{2+} \rightarrow Hg_2{}^{2+}$ reduction, driven chemically (with the help of PDAN/CNT in the first scan) or electrochemically (under more negative potential bias in the second scan).

As for Cu^{2+} ($E^0{}_{Cu2+/Cu} = +0.101$ V), its detection seems impossible within given potential range (0 V to +0.7 V), when the adsorption step was done at room temperature whereas at a higher temperature (80 °C), a significant SWV peak was recorded at +0.6 V (Fig. 6). From thermodynamic viewpoint, in virtue of Nerst equation ($E(Cu^{2+}/Cu) = E^0(Cu^{2+}/Cu) + RT/nF \times \ln([Cu^{2+}])$ the potential varies negligibly when temperature increases from ambient to 80 °C. On the other side, from kinetic viewpoint, the adsorption may be accelerated/intensified with increasing temperature and Cu^{2+} amount might be accumulated sufficiently to be reduced pronouncedly ($Cu^{2+} \rightarrow Cu$). Thus, Cu^{2+} detection is possible by SWV as experimentally confirmed in Fig. 6.

As for other M^{2+}, due to their E^0 values, within given potential range, they cannot be detected, because neither they can be accumulated nor sufficiently accumulated to be detected within above potential range [24–26].

In order to obtain a more sensitive detection of Hg^{2+} (*i.e.* maximized analytical SWV signal) a systematic optimization of the experimental parameters affecting the SWV response such as frequency, pulse amplitude and scan increment was carried out. It was found out that a frequency of 12.5 Hz, a scan increment of 8 mV, a pulse amplitude of 25 mV and a scanning potential range from 0.0 V to +0.7 V are the most appropriate. Furthermore, it is well known that the effect of the pH may affect the protonation

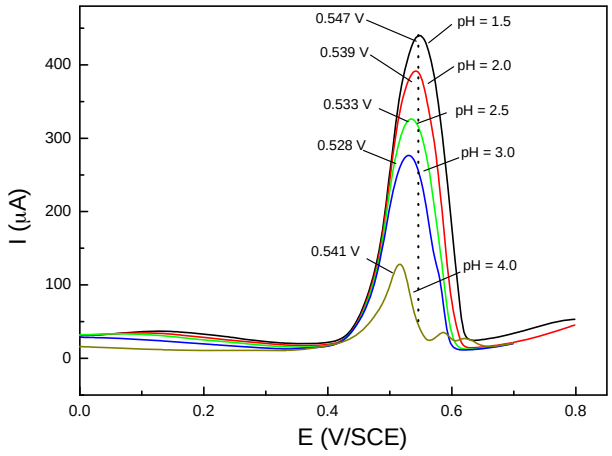

Fig. 7. pH dependence of SWV curves, registered during Hg^{2+} detection.

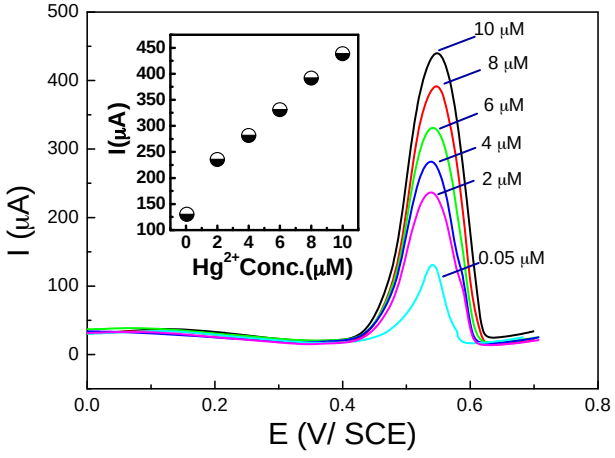

Fig. 8. SWV curves, registered during Hg^{2+} detection at different concentrations (0.05–10 μM) and corresponding calibration curve (inset).

and therefore complexation capacity and the detection sensitivity in overall. In order to check it, current intensity (I_p) was examined from 4.0 to 1.5. It was revealed that the peak potential was strongly pH-dependent and that the peak current decreases from pH 1.5 to 4.0, as shown in Fig. 7. Some comments on pH effect can be made. First, as reported in literature, the lower pH the lower adsorption capacity of M^{2+}, due to competition between chelate forming groups and H^+ on the same sites of coordination in the solution. Second, according to Nernst equation low pH value can make redox couple of $Hg^{2+}/Hg_2{}^{2+}$ more powerfully oxidizing, rending its peak intensity and corresponding potential value on abscissa more intensive and more positive respectively, as observed experimentally. Thus, for the analytical purpose, all subsequent experiments were carried out at pH 1.5 to obtain the maximized analytical SWV signal.

Fig. 8 presents responses of the fabricated IDA sensor to different concentrations of Hg^{2+} under optimized experimental conditions. The calibration curve, evaluated by the interpolation of the current intensity values of each concentration (0–10 μM of Hg^{2+}) in the standard calibration curve, is shown in the upper left inset of this figure. The performance of the proposed voltammetric detection of Hg was also checked by AAS experiment and it was in good agreement with AAS method for all tested concentrations (figure not shown).

4. Conclusion

An easy synthesis of PDAN/CNT interface for a sensitive detection of Hg^{2+} based on IDA was proposed. To investigate the selectivity of this method, other interference M^{2+} ions have been tested. The obtained results indicated the potential ability of PDAN/CNT IDA design for Hg^{2+} detection (and Cu^{2+} in less extent) by SWV. As for the detection principle, it is proposed that oxidizing characteristic of redox potential (E^0) with the respect to that of PDAN/CNT resulted in sensitive signal transduction of Hg^{2+}. One advantageous aspect of IDA is the ability to detect simultaneously multiple analyses, so this approach has proved to be an inexpensive, efficient method to simultaneous ion metal detection and this IDA type electrode on PDAN/CNT platform can extend its utility in many other sensing applications.

Acknowledgements

Funding of this work was provided by Viet Nam National Foundation for Science and Technology Development NAFOSTED grant (104.03-2010.60). L.D. Tran and D.T. Nguyen acknowledge Department of International Cooperation, VAST for additionally financial support to their working visit to ITODYS, University of Paris Diderot, France (VAST- CNRS cooperation framework). The authors sincerely acknowledge Prof. M.C. Pham (ITODYS) for her useful discussion and reading to an early version of this manuscript.

Appendix A. Supplementary data

Supplementary data associated with this article can be found, in the online version, at doi:10.1016/j.talanta.2011.07.094.

References

[1] S.d. Flora, C. Bennicelli, M. Bagnasco, Mutation Research/Reviews in Genetic Toxicology 317 (1) (1994) 57–79.
[2] Edition of the Drinking Water Standards and Health Advisories, *EPA* 820-*R*-11-002, Office of Water, United States Environmental Protection Agency, 2011.
[3] K. Leopold, M. Foulkes, P. Worsfold, Analytical Chimica Acta 663 (2010) 127–138.
[4] Y. Cai, Trends in Analytical Chemistry 19 (1) (2000) 62–66.
[5] C.-W. Liu, C.-C. Huang, H.-T. Chang, Analytical Chemistry 81 (2009) 2383–2387.
[6] K. Wu, S. Hu, J. Fei, W. Bai, Analytica Chimica Acta 489 (2003) 215–221.
[7] M.L. Tercier, J. Buffle, Electroanalysis 5 (1993) 187–200.
[8] C. Locatelli, Electroanalysis 9 (1997) 1014–1017.
[9] S.M. Park, in: H.S. Nalwa (Ed.), Handbook of Organic Conductive Molecules and Polymers, vol. 3, Wiley, Chichester, UK, 1997.
[10] M.C. Pham, M. Oulahyne, M. Mostefai, M.M. Chehimi, Synthetic Metals 93 (1998) 89–96.
[11] A. Meneguzzi, M.C. Pham, J.C. Lacroix, B. Piro, A. Adenier, C.A. Ferreira, P.C. Lacaze, Journal of the Electrochemical Society 148 (2001) B121–B126.
[12] A. Kudelski, J. Bukowska, K. Jackowska, Journal of Molecular Structure 482–483 (1999) 291–294.
[13] X.-G. Li, M.-R. Huang, S.-X. Li, Acta Materialia 52 (2004) 5363–5374.
[14] B.K. Jena, C.R. Raj, Analytical Chemistry 80 (2008) 4836–4844.
[15] H. Xu, L.P. Zeng, S.J. Xing, G.Y. Shi, Y.Z. Xian, L.T. Jin, Electrochemistry Communications 10 (2008) 1839–1843.
[16] J. Gong, T. Zhou, D. Song, L. Zhang, Sensors and Actuators B: Chemical 150 (2010) 491–497.
[17] S.J.R. Prabakar, C. Sakthivel, S. Sriman Narayanan, Talanta 1 (2011) 290–297.
[18] A. Safavi, E. Farjami, Analytica Chimica Acta 688 (2011) 43–48.
[19] E. Bernalte, C. Marín Sánchez, E. Pinilla Gil, Analytica Chimica Acta 689 (2011) 60–64.
[20] B.J. Patys, M. Skompska, K. Jackowska, Journal of Electroanalytical Chemistry 433 (1997) 41–48.
[21] J. Rutkowska, K. Kilian, K. Pyrzynska, European Polymer Journal 44 (2008) 2108–2114.
[22] K. Kilian, K. Pyrzynska, Reactive & Functional Polymers 68 (2008) 974–980.
[23] R. Agaz, M.T. Sevilla, L. Hernandez, Analytica Chimica Acta 15 (1993) 205–212.
[24] S.A. Mahesar, S.T.H. Sherazi, A. Niaz, M.I. Bhanger, Sirajuddin, A. Rauf, Food and Chemical Toxicology 48 (2010) 2357–2360.
[25] C. Kokkinos, A. Economou, I. Raptis, T. Speliotis, Electrochemistry Communications 11 (2009) 250–253.
[26] P. Miao, L. Liu, Y. Li, G. Li, Electrochemistry Communications 11 (2009) 1904–1907.